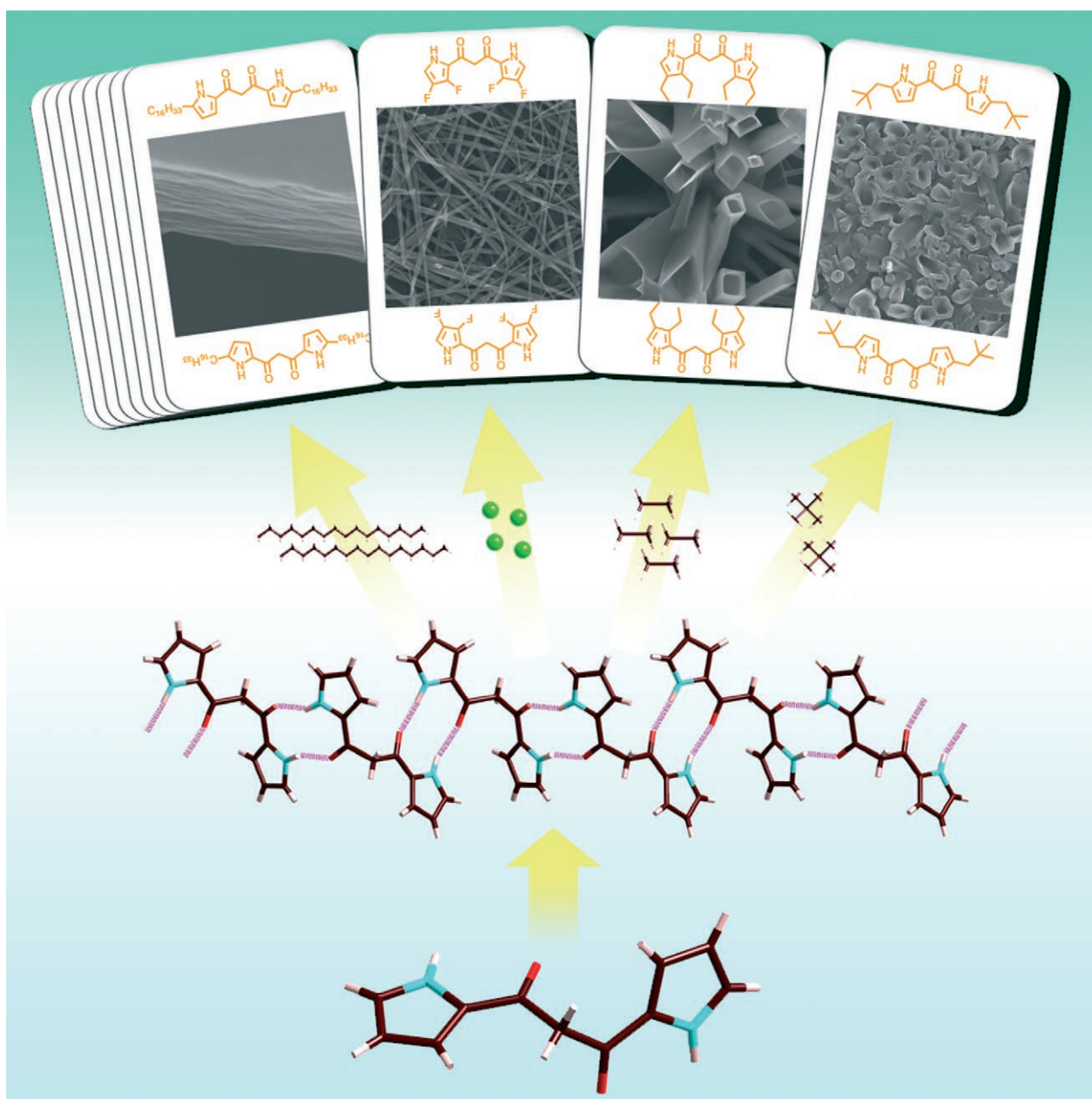


Micro- and Nanometer-Scale Porous, Fibrous, and Sheet Architectures Constructed by Supramolecular Assemblies of Dipyrrolyldiketones

Hiromitsu Maeda,*^[a, b] Yukio Kusunose,^[a] Masahiro Terasaki,^[a] Yoshihiro Ito,^[a] Chikoto Fujimoto,^[a] Rika Fujii,^[a] and Takashi Nakanishi*^[c]



Abstract: X-ray analysis of some 1,3-dipyrrolyl-1,3-propanediones synthesized from pyrroles and malonyl chloride derivatives revealed 1D supramolecular networks formed by N–H...O=C interactions in the solid state. Micro- and nanometer-scale morphologies of porous, fibrous, and sheet structures were fabricated by hydrogen-

bonding interactions and determined by fine-tuning the substituents and the solvents used. Of the unique poly-

Keywords: hydrogen bonds • nanostructures • polymorphism • self-assembly • supramolecular chemistry

morphs, ordered 2D lamellar sheet structures of the derivatives with long alkyl chains (C₁₆H₃₃, C₁₄H₂₉, and so on) were constructed by van der Waals hydrophobic effects between aliphatic chains as well as hydrogen bonding.

Introduction

Well-defined micro- and nanometer-sized architectures fabricated by self-assembled organic molecules have attracted much attention due to their properties as potential functional materials.^[1–7] For example, supramolecular nanofibers were observed in gelled materials consisting of low-weight organic molecules,^[3,4] and sheetlike morphologies were fabricated from amphiphilic lipid bilayers.^[1b] Furthermore, supramolecular nanotubes were formed by transformation from sheet structures via twisted and coiled ribbons based on amphiphilic molecules such as glucosides with long alkyl chains.^[5] Similarly, amphiphilic hexa-*peri*-hexabenzocoronenes self-assemble to form π -electronic, discrete nanotubular objects.^[6] In contrast to such nanoscale objects, larger tube- and pipelike structures were also provided based on the organization and crystallization of small organic molecules.^[7]

Among versatile weak interactions, hydrogen-bonding and hydrophobic interactions are essential for the construction of supramolecular structures, such as DNA double helices and protein subunits, in biological systems.^[8] Although amide NH and CO sites in proteins usually orientate to opposite sides, NH and CO moieties bridged by one sp² carbon atom on the same plane exhibit the double hydrogen-bonding interactions appropriate for self-organization.

Pyrrole, a π -conjugated heterocycle found in functional dyes such as heme and chlorophyll,^[9] behaves as a hydrogen-bonding donor due to its polarized NH group. To date, various types of cyclic and acyclic anion receptors consisting of pyrrole ring(s) have been synthesized.^[10] Furthermore, self-assembled supramolecular networks of acyclic pyrrole derivatives with carbonyl groups at α positions have been observed in the solid state as well as in solution.^[11–13] For example, bis(ethoxycarbonyl)-substituted terpyrrole constructs a 1D network by using N–H...O=C interaction.^[11a] However, micro- and nanometer-scale materials based on acyclic pyrrole derivatives have not yet been reported. Herein, dimension-controlled micro- and nanometer-scale structures based on the hydrogen-bonding interactions of dipyrrolyldiketones are reported. To the best of our knowledge, this is the first report on nanostructures, especially those with sheetlike morphology, involving the hydrogen-bond-donating NH group of acyclic oligopyrroles combined with fine-tuning of the substitution pattern.

Results and Discussion

Synthesis and Hydrogen-Bonding Self-Assemblies of Dipyrrolyldiketones

1,3-Dipyrrolyl-1,3-propanediones (**1a–e**, **2a–d**, **3a**, **3b**, **4a**, **4b**), with or without alkyl substituents at the pyrrole periphery and bridging methylene units, have been synthesized in modest yields from pyrroles and malonyl chloride deriva-

[a] Prof. Dr. H. Maeda, Y. Kusunose, M. Terasaki, Y. Ito, C. Fujimoto, R. Fujii
Department of Bioscience and Biotechnology
Faculty of Science and Engineering
Ritsumeikan University
Kusatsu 525-8577 (Japan)
Fax: (+81) 77-561-2659
E-mail: maedahir@se.ritsumeik.ac.jp

[b] Prof. Dr. H. Maeda
Department of Applied Molecular Science
Institute for Molecular Science (IMS)
Okazaki 444-8787 (Japan)

[c] Dr. T. Nakanishi
Organic Nanomaterials Center (ONC) and
International Center for Young Scientists (ICYS)
National Institute for Materials Science (NIMS)
Tsukuba 305-0044 (Japan)
Fax: (+81) 29-860-4706
E-mail: Nakanishi.Takashi@nims.go.jp


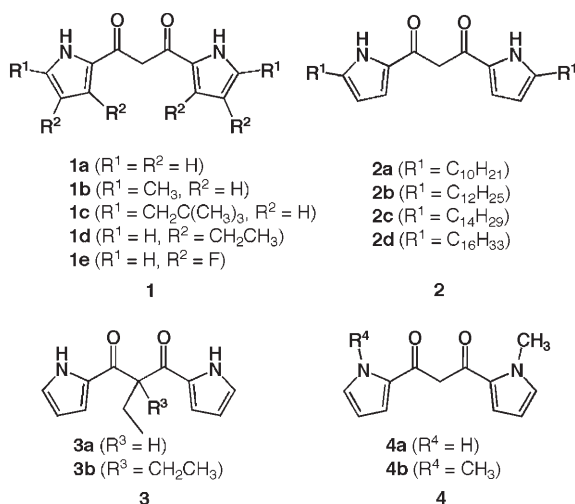
 Supporting information for this article is available on the WWW under <http://www.chemasianj.org> or from the author.

Table 1. Summary of crystallographic data for **1a**, **1d**, **3a**, **3b**, and **4b**.

	1a	1d	3a	3b	4b
Formula	C ₁₁ H ₁₀ N ₂ O ₂	C ₁₉ H ₂₆ N ₂ O ₂	C ₁₃ H ₁₄ N ₂ O ₂	C ₁₅ H ₁₈ N ₂ O ₂	C ₁₃ H ₁₄ N ₂ O ₂
FW	202.21	314.42	230.26	258.31	230.26
Crystal size [mm]	0.70 × 0.10 × 0.10	0.30 × 0.20 × 0.20	0.40 × 0.30 × 0.20	0.35 × 0.20 × 0.15	0.60 × 0.35 × 0.30
Crystal system	triclinic	monoclinic	monoclinic	monoclinic	orthorhombic
Space group	<i>P</i> $\bar{1}$ (no. 2)	<i>P</i> 2 ₁ / <i>n</i> (no. 14)	<i>C</i> 2/ <i>c</i> (no. 15)	<i>P</i> 2 ₁ / <i>n</i> (no. 14)	<i>F</i> dd2 (no. 43)
<i>a</i> [Å]	8.500(13)	11.444(4)	13.4259(16)	11.9213(15)	18.3896(14)
<i>b</i> [Å]	10.355(14)	10.861(4)	8.8327(11)	8.9492(11)	26.778(2)
<i>c</i> [Å]	11.837(13)	14.563(8)	20.209(2)	13.3176(17)	4.7968(4)
α [°]	67.11(4)	90	90	90	90
β [°]	86.56(5)	107.135(16)	102.601(2)	102.097(2)	90
γ [°]	85.39(5)	90	90	90	90
<i>V</i> [Å ³]	956(2)	1729.6(13)	2338.8(5)	1389.3(3)	2362.1(3)
ρ_{calcd} [g cm ⁻³]	1.405	1.207	1.308	1.235	1.295
<i>Z</i>	4	4	8	4	8
<i>T</i> [K]	123(2)	123(2)	90(2)	90(2)	90(2)
Reflections	9414	15 942	6973	8297	3504
Unique reflections	4330	3909	2656	3160	1338
Variables	272	212	159	174	79
$\lambda(\text{MoK}\alpha)$ [Å]	0.71075	0.71075	0.71073	0.71073	0.71073
<i>R</i> 1	0.0379 (<i>I</i> > 2 σ (<i>I</i>))	0.0546 (<i>I</i> > 2 σ (<i>I</i>))	0.0394 (<i>I</i> > 2 σ (<i>I</i>))	0.0577 (<i>I</i> > 2 σ (<i>I</i>))	0.0320 (<i>I</i> > 3 σ (<i>I</i>))
<i>wR</i> 2	0.0840 (<i>I</i> > 2 σ (<i>I</i>))	0.1480 (<i>I</i> > 2 σ (<i>I</i>))	0.0996 (<i>I</i> > 2 σ (<i>I</i>))	0.1203 (<i>I</i> > 2 σ (<i>I</i>))	0.0836 (<i>I</i> > 3 σ (<i>I</i>))
GO F	0.890	1.038	1.011	1.066	1.105



tives in CH₂Cl₂.^[14–16] Starting α -alkylpyrroles for **1b**, **1c**, and **2a–d** were prepared by acylation (or formylation) of unsubstituted pyrrole followed by reduction of the carbonyl group

Abstract in Japanese:

1,3-ジピロリル-1,3-プロパンジオン誘導体のX線結晶構造解析から、固体状態におけるN–H⋯O=C間の相互作用による1次元超分子ネットワーク構造が明らかとなった。さらに、水素結合および側鎖間の相互作用を基盤とし、周辺置換基に依存したチューブやファイバー、シートなどの多様なマイクロ・ナノメータースケール組織構造の形成が電子顕微鏡観察によって確認された。

to a methylene unit.^[17–20] In solution, dipyrrolyldiketones exist as equilibrium mixtures of enol tautomers.

Single-crystal X-ray analysis of the dipyrrolyldiketones (Table 1) revealed that the keto forms are more stable in the solid state. Furthermore, unsubstituted **1a**, β -ethyl-substituted **1d**, and bridging-C alkyl **3a** and **3b** form 1D intermolecular hydrogen-bonding assemblies by using the NH and CO moieties at the edges of each molecule (Figure 1a–d). Regularly assembled structures are repeated by every two molecules in **1a**, **1d**, and **3b** and by every four in **3a**. Diketones **1a**, **1d**, and **3b**, which are chiral owing to the twisted methylene (CH₂) unit, interact with neighboring enantiomers to afford *RSRS*⋯ racemic strands. In the case of ethyl-substituted **3a**, chiral pairs of molecules are associated with neighboring ones as *RRSSRR*⋯. The intramolecular dihedral angles between two planes consisting of five atoms (NH and CO with the bridging α -C) were estimated to be 109.01 (102.67 for another conformation), 17.26, 81.32, and 97.75° for **1a**, **1d**, **3a**, and **3b**, respectively. Of these diketones, β -ethyl-substituted **1d** forms a rather planar geometry to afford the hydrogen-bonding arrays (Figure 1b). In sharp contrast to **1d**, *N*-methyl-substituted derivative **4b** shows an almost-perpendicular corresponding angle (89.62°) and a packing diagram without hydrogen-bonding interaction in the solid state (Figure 1e).

Polymorphs of Dipyrrolyldiketone Derivatives

Various self-organizations of diketones observed in X-ray structures make possible the fabrication of micro- and nano-meter-sized objects identified by scanning electron microscopy (SEM). The objects from CH₂Cl₂ were rapidly fabricated by evaporation of the solvent. Unsubstituted and methyl-

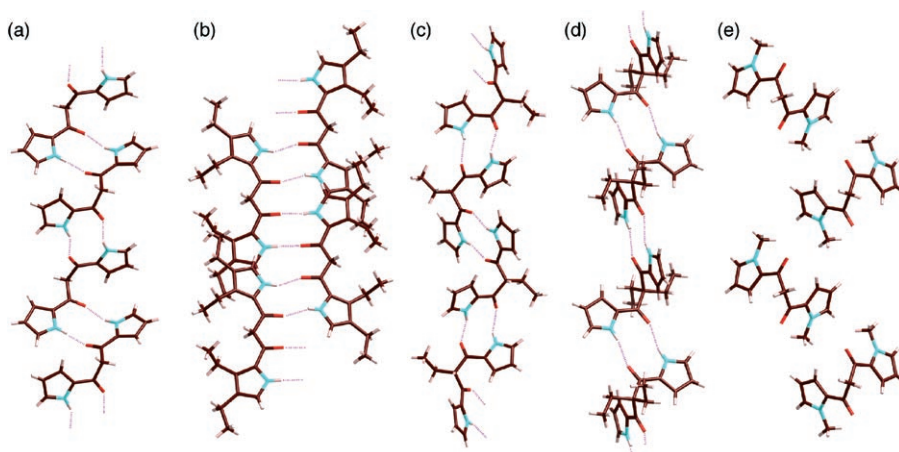


Figure 1. Self-assemblies of a) **1a**, b) **1d**, c) **3a**, d) **3b**, and e) packing diagram of **4b** in the solid state. Atom color code: brown, pink, blue, and red refer to carbon, hydrogen, nitrogen, and oxygen, respectively.

substituted diketones **1a** and **1b** formed the rather crystalline flowerlike and plate morphologies, respectively, from CH_2Cl_2 on a scale several tens of micrometers large. In contrast, neopentyl-substituted derivative **1c** formed hexagonal tubes with pores^[7a] 0.5–4 μm diagonally across and lengths of 10–20 μm from the same solvent (Figure 2a). Smaller ob-

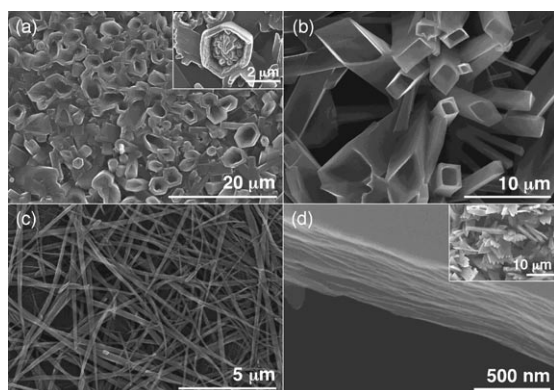


Figure 2. SEM images of a) **1c** (inset: hexagonal pore), b) **1d**, c) **1e**, and d) **2d** (inset: assemblies of nanosheets). The samples were prepared by casting of the solution in CH_2Cl_2 onto silicon substrate.

jects also grew within some of the porous spaces (Figure 2a, inset). Similarly, β -ethyl-substituted **1d** formed tube structures with rectangular and parallelogram pores 1–4 μm diagonally across (Figure 2b). The formation mechanism of such polygonal microporous structures includes the condensation and organization of organic molecules by evaporation of solvent, similar to that of primary aromatic amide with long aliphatic chains,^[7c] but differs

from the case of transformation via the intermediate sheet and ribbon structures.^[5,6]

On the other hand, β -fluorinated **1e** afforded fibers 0.1–0.3 μm wide (Figure 2c). Furthermore, **2d**, with a long hexadecyl ($\text{C}_{16}\text{H}_{33}$) chain, formed assemblies of thin-layer stacking sheets from CH_2Cl_2 (Figure 2d). In contrast to all these observations, **4a** and fully N-blocked **4b** formed nontextural and random rocklike structures, respectively, due to the absence of multiple hydrogen-bonding interactions. As seen in the rather less-ordered structures of **1a** and **1b**, adequate alkyl

chains or substituents are effective for the fabrication of micro- and nanometer-scale polymorphs.

Less-polar *n*-hexane also gave sheet structures for alkyl-substituted diketones **2a–d** similar to those with CH_2Cl_2 . In sharp contrast, for other diketones such as α -neopentyl **1c**, β -ethyl **1d**, and β -fluoro **1e**, the morphologies of the nanoarchitectures were tuned by the solvents used.^[21] For example, **1c** formed fibers approximately 0.4 μm wide from *n*-hexane. Moreover, β -substituted **1d** and **1e** provided rock- and swordlike objects, respectively. At present, the effect of solvents is not highlighted in detail, although it is useful for controlling the shapes of ordered structures.

Transmission electron microscopy (TEM) and optical microscopy (OM) images also illustrated the tubes, sheets, and fibers of the diketones (Figure 3). Interestingly, β -fluoro-substituted **1e** formed thinner fibers 10–50 nm wide under conditions similar to those of the SEM measurements (Figure 3a).

Besides hydrogen bonding, van der Waals interactions between the alkyl chains also provide the versatile morphologies as observed by SEM, TEM, and OM. The fibers and sheets^[1b] are the results of the 1D and 2D orientations of the self-assembled diketones. The polymorphs from CH_2Cl_2 , in which the diketone derivatives are soluble as a monomer, were fabricated during rapid evaporation of the solvent on the substrate to afford microcrystals (hexagonal and parallelogram tubes) or regularly ordered assemblies (fibers and

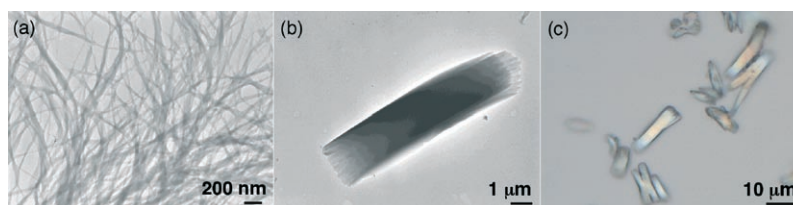


Figure 3. TEM images of a) **1e** and b) **2d** from CH_2Cl_2 without staining and c) OM images of **2d** from *n*-hexane.

sheets). On the other hand, micro- and nanometer-scale objects from *n*-hexane, such as sheets of alkyl-substituted derivatives **2a–d**, were constructed in the solvent.

Organized Structures Correlated with X-ray Diffraction Analysis

Organized structures of dipyrrolyldiketones are modulated by peripheral substituents and a flexible bridging CH₂ unit. However, micro- and nanometer-scale morphologies, the tubelike architectures of **1c** and **1d** (Figure 2a and b), and the nanofibers of **1e** (Figure 2c) can be correlated with and explained by the single-crystal X-ray structures (Figure 1) as well as X-ray diffraction (XRD) analysis. The XRD pattern of α -neopentyl-substituted **1c**, with peaks at $2\theta = 7.07$ (100), 12.12 (110), 14.00 (200), 18.40 (210), and 21.02° (300), can be indexed according to the simulated pattern based on hexagonal packing in the solid state, as seen in the supramolecular self-assembled porphyrin hollow nanoprism.^[7a] On the other hand, in the case of β -ethyl **1d**, although the XRD pattern is very complicated, presumably owing to the multicrystalline system, the peaks at $2\theta = 10.21$ (011), 11.85 (−111), 15.05 (012), and 20.46° (022) can be assigned by simulation based on the crystal data (Figure 1b). Furthermore, the XRD pattern of β -fluoro **1e**, with peaks at $2\theta = 10.44$ (100), 12.89 (101), 14.91 (−111), 18.68 (020), 21.09 (122), and 30.04° (−222), may be indexed according to the simulated pattern from X-ray data of unsubstituted **1a** (Figure 1a), which suggests that **1e** has a rather similar molecular-packing structure to **1a** resulting in fibrous structures.

Nanosheets of the Diketones with Long Alkyl Chains

Dipyrrolyldiketones **2a–d** are amphiphilic building blocks with hydrophilic NH and CO units and hydrophobic long alkyl chains attached to the ends of the core units. Aliphatic substituents such as C₁₆H₃₃, C₁₄H₂₉, and so on interact with each other to form organized assemblies. Therefore, as seen above, **2a–d** formed ordered structures of nanoscale sheets, whose orientations at the molecular-assembly level were investigated.

The XRD patterns of **2a–d**, obtained by a cast film from *n*-hexane at room temperature, reveal ordered layer structures with similar diffraction patterns from (001) to (004) (Figure 4a for **2d**). The estimated XRD *d*-spacing values of **2a–d** were 2.60, 2.97, 3.32, and 3.66 nm, respectively. These values are consistent with regular 1D arrangements (Figure 4b for **2d**) and indicate control of the layer distances by the alkyl-chain lengths. The Δd values between those of C_{*n*}H_{2*n*+1} and C_{*n*+2}H_{2*n*+5}-substituted derivatives were 0.34–0.37 nm; these values were derived from the length of two ethylene (C₂H₄) units and are affected by the tilt of the diketone molecules in the assemblies as well as the dihedral angles between two alkyl chains. In the case of a theoretical study of a single molecule at the AM1 level,^[22] the intramolecular distances between the terminal carbon atoms of the alkyl chains were estimated to be 2.73, 3.15, 3.57, and

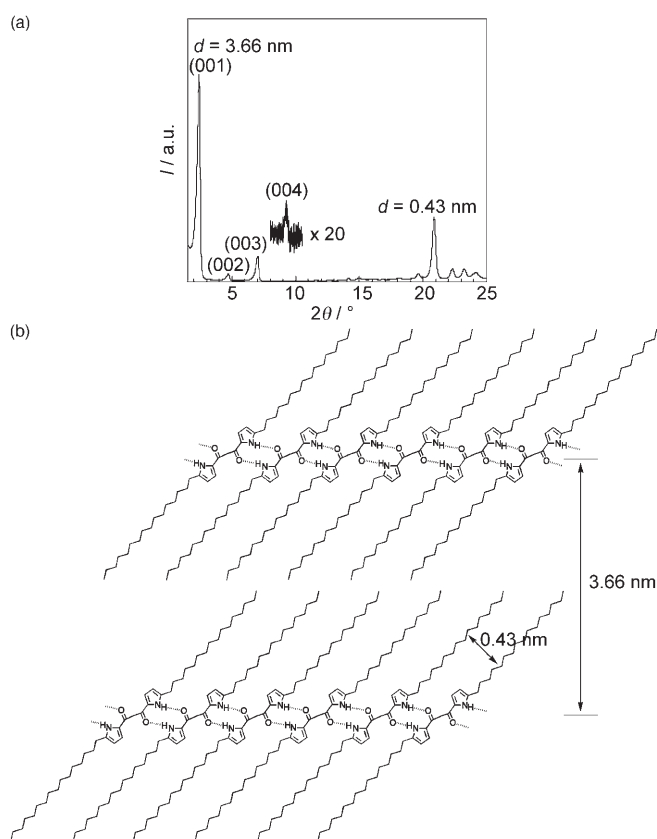


Figure 4. a) XRD data of **2d** from *n*-hexane. b) Schematic representation of the possible ordered arrangement of the assembly of **2d**.

4.00 nm for **2a–d**, respectively, which afforded Δd values of 0.42–0.43 nm, a little larger than those observed by XRD. Furthermore, diketone **2d** showed an ordered distance of 0.43 nm estimated from the peak at $2\theta = 20.9^\circ$, which is possibly derived from the close-packing of the alkyl chains. Similar trends were observed in the other derivatives **2a–c**. From the above observations, the existence of well-organized multilayer structures is clear.

Atomic force microscopy (AFM) of **2d** on silicon substrate suggests that the microstructures are in the form of nanosheets 20–30 nm thick (Figure 5); this was also inferred from SEM (Figure 2d, inset). Furthermore, IR spectra of cast film from *n*-hexane displayed CH₂ stretching vibrations at 2849.4 ($\tilde{\nu}_{\text{sym}}$) and 2917.8 cm^{−1} ($\tilde{\nu}_{\text{asym}}$) for **2d**, which indicate the all-*trans* geometry of the alkyl units. In the case of **2a–c**, *trans*-rich geometries were suggested by the corresponding IR peaks at 2850.6 ($\tilde{\nu}_{\text{sym}}$) and 2918.6 cm^{−1} ($\tilde{\nu}_{\text{asym}}$). Stretching peaks of the hydrogen-bonding sites (NH and CO) of **2d** were observed at 3279.2 (NH) and 1637.3 cm^{−1} (CO), which confirm the presence of N–H⋯O=C hydrogen-bonding interactions. The derivatives with shorter alkyl chains, **2a–c**, showed the NH stretching at 3265.3 (**2a**), 3273.9 (**2b**), and 3276.4 cm^{−1} (**2c**), suggesting that van der Waals interactions between aliphatic moieties would weaken the hydrogen bonding. In other words, rather weak hydrophobic effects by shorter alkyl groups could be compensated for by the more-

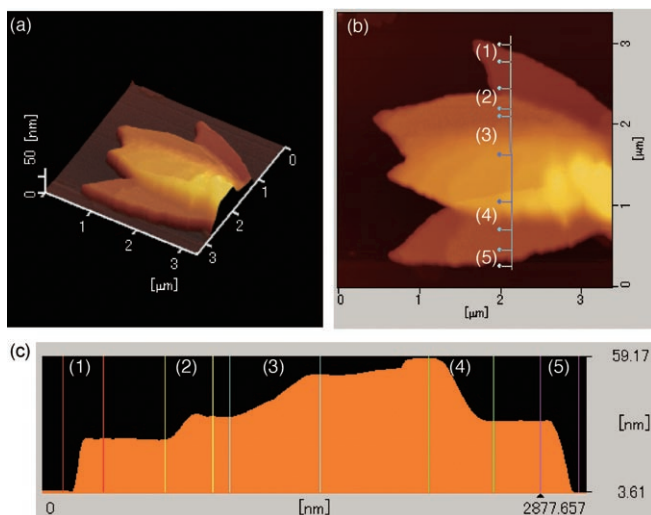


Figure 5. AFM in dynamic force mode of α -hexadecyl-substituted diketone **2d** on silicon substrate. a) 3D image, b) 2D image, and c) cross-sectional analysis. Height differences are 1) 21.3, 2) 9.5, 3) 17.4, 4) 25.8, and 5) 29.2 nm. The sample was prepared by dropping a 0.02 mM solution in *n*-hexane onto the silicon surface.

effective N–H \cdots O=C interactions. All the SEM, XRD, AFM, and IR data support the ordered 2D lamellar sheet structures.

Conclusions

In summary, to form supramolecular micro- and nanometer-scale objects based on C_3 -bridged oligopyrroles, the polarized pyrrole NH group with a carbonyl moiety at the neighboring α -position is suitable as a scaffold for hydrogen-bonding interactions.^[11d] Facile fine-tuning of peripheral substituents affords functionalized micro- and nanometer-scale materials with versatile morphologies of choice, which could be utilized, for example, as light-transmitting wires in the case of fibers. The formation mechanisms of these architectures could also be clarified based on more libraries of dipyrrolyldiketones. Investigations into both solvent effects to determine the shapes of the nanoarchitectures and guest recognition of the tubular objects are currently under way.

Experimental Section

General Procedures

Starting materials were purchased from Wako Chemical Co., Nacalai Chemical Co., and Aldrich Chemical Co. and used without further purification unless otherwise stated. UV/Vis spectra were recorded on a Hitachi U-3500 spectrometer. NMR spectra used in the characterization of products were recorded on JEOL AL-400 400 MHz and JEOL ECA-600HR 600 MHz spectrometers. All NMR spectra were referenced to the solvent. Fast atom bombardment mass spectrometric studies (FABMS) were made with a JEOL-HX110 instrument in positive-ion mode with a 3-nitrobenzylalcohol matrix. TLC analysis was carried out on aluminum sheets coated with silica gel 60 (Merck 5554). Column chromatography

was performed on Sumitomo alumina KCG-1525, Wakogel C-200, C-300, and Merck silica gel 60 and 60H.

Syntheses

1b: In a similar manner to the literature procedure,^[14,16] a solution of 2-methylpyrrole^[17,18] (329 mg, 4.1 mmol) in CH_2Cl_2 (60 mL) was treated with malonyl chloride (286 mg, 2.0 mmol) at 0°C and stirred for 2.5 h at the same temperature. After consumption of the starting pyrrole was confirmed by TLC analysis, the mixture was washed with saturated aqueous Na_2CO_3 and water, dried over anhydrous Na_2SO_4 , filtered, and evaporated to dryness. The residue was then subjected to flash chromatography over silica gel (eluent: 2% MeOH/ CH_2Cl_2) and recrystallized from CH_2Cl_2 /hexane to afford **1b** (155.3 mg, 33%) as a pale-yellow solid. R_f = 0.40 (5% MeOH/ CH_2Cl_2); 1H NMR (400 MHz, $CDCl_3$, 27°C): δ = 9.23 (brs, 2H, NH), 6.97 (s, 2H, pyrrole-H), 5.99 (s, 2H, pyrrole-H), 4.10 (s, 2H, CH_2), 2.29 ppm (s, 6H, CH_3); MS (FAB): m/z (%) calcd for $C_{13}H_{14}N_2O_2$: 230.11 $[M]^+$; found: 230.0 (55) $[M]^+$, 231.0 (100) $[M+1]^+$.

2a: A solution of 2-decylpyrrole^[19,20] (311.7 mg, 1.5 mmol) in CH_2Cl_2 (5 mL) was treated with malonyl chloride (105.7 mg, 0.75 mmol) at 0°C and stirred for 3.5 h at the same temperature. After consumption of the starting pyrrole was confirmed by TLC analysis, the mixture was washed with saturated aqueous Na_2CO_3 and water, dried over anhydrous Na_2SO_4 , filtered, and evaporated to dryness. The residue was then subjected to chromatography over silica gel (Wakogel C-300, eluent: 1% MeOH/ CH_2Cl_2) and recrystallized from CH_2Cl_2 /hexane to afford **2a** (95.9 mg, 27%) as a white solid. R_f = 0.20 (1% MeOH/ CH_2Cl_2); 1H NMR (400 MHz, $CDCl_3$, 27°C): δ = 9.05 (brs, 2H, NH), 6.99 (s, 2H, pyrrole-H), 6.01 (s, 2H, pyrrole-H), 4.11 (s, 2H, CH_2), 2.59 (t, J = 7.6 Hz, 4H, alkyl-H), 1.37–1.20 (m, 32H, alkyl-H), 0.88 ppm (t, J = 6.6 Hz, 6H, alkyl-H); MS (FAB): m/z (%) calcd for $C_{31}H_{50}N_2O_2$: 482.39 $[M]^+$; found: 482.4 (55) $[M]^+$, 483.3 (100) $[M+1]^+$.

2b: A solution of 2-dodecylpyrrole^[19,20] (394 mg, 1.67 mmol) in CH_2Cl_2 (10 mL) was treated with malonyl chloride (118.4 mg, 0.84 mmol) at 0°C and stirred for 3 h at the same temperature. After consumption of the starting pyrrole was confirmed by TLC analysis, the mixture was washed with saturated aqueous Na_2CO_3 and water, dried over anhydrous Na_2SO_4 , filtered, and evaporated to dryness. The residue was then subjected to chromatography over silica gel (Wakogel C-300, 200, 60, eluent: 2% MeOH/ CH_2Cl_2) and recrystallized from CH_2Cl_2 /hexane to afford **2b** (114.1 mg, 25%) as a white solid. R_f = 0.70 (5% MeOH/ CH_2Cl_2); 1H NMR (400 MHz, $CDCl_3$, 27°C): δ = 9.06 (s, br, 2H, NH), 6.98 (s, 2H, pyrrole-H), 6.01 (s, 2H, pyrrole-H), 4.11 (s, 2H, CH_2), 2.59 (t, J = 7.6 Hz, 4H, alkyl-H), 1.36–1.19 (m, 40H, alkyl-H), 0.88 ppm (t, J = 6.8 Hz, 6H, alkyl-H); FABMS: m/z (%) calcd for $C_{35}H_{58}N_2O_2$ $[M]^+$: 538.45; found: 538.5 (60) $[M]^+$, 539.5 (100) $[M+1]^+$.

2c: A solution of 2-tetradecylpyrrole^[19,20] (124.4 mg, 0.47 mmol) in CH_2Cl_2 (10 mL) was treated with malonyl chloride (33.8 mg, 0.24 mmol) at 0°C and stirred for 3 h at the same temperature. After consumption of the starting pyrrole was confirmed by TLC analysis, the mixture was washed with saturated aqueous Na_2CO_3 and water, dried over anhydrous Na_2SO_4 , filtered, and evaporated to dryness. The residue was then subjected to chromatography over silica gel (Wakogel C-300, 200, eluent: 1% MeOH/ CH_2Cl_2) and recrystallized from CH_2Cl_2 /hexane to afford **2c** (35.6 mg, 25%) as a white solid. R_f = 0.20 (1% MeOH/ CH_2Cl_2); 1H NMR (400 MHz, $CDCl_3$, 27°C): δ = 9.08 (brs, 2H, NH), 6.98 (s, 2H, pyrrole-H), 6.01 (s, 2H, pyrrole-H), 4.10 (s, 2H, CH_2), 2.59 (t, J = 7.6 Hz, 4H, alkyl-H), 1.36–1.20 (m, 48H, alkyl-H), 0.88 ppm (t, J = 6.8 Hz, 6H, alkyl-H); MS (FAB): m/z (%) calcd for $C_{39}H_{66}N_2O_2$: 594.51 $[M]^+$; found: 594.5 (64) $[M]^+$, 595.5 (100) $[M+1]^+$.

2d: A solution of 2-hexadecylpyrrole^[19,20] (582 mg, 2.0 mmol) in CH_2Cl_2 (30 mL) was treated with malonyl chloride (141 mg, 1.0 mmol) at 0°C and stirred for 2 h at the same temperature. After consumption of the starting pyrrole was confirmed by TLC analysis, the mixture was washed with saturated aqueous Na_2CO_3 and water, dried over anhydrous Na_2SO_4 , filtered, and evaporated to dryness. The residue was then subjected to flash chromatography over silica gel (eluent: 3% MeOH/ CH_2Cl_2) and recrystallized from $CHCl_3$ /hexane to afford **2d** (193.3 mg, 30%) as a white solid. R_f = 0.70 (5% MeOH/ CH_2Cl_2); 1H NMR

(400 MHz, CDCl_3 , 27°C): δ = 9.10 (brs, 2H, NH), 7.00 (s, 2H, pyrrole-H), 6.02 (s, 2H, pyrrole-H), 4.11 (s, 2H, CH_2), 2.60 (t, J = 8.0 Hz, 4H, alkyl-H), 1.30–1.23 (m, 56H, alkyl-H), 0.88 ppm (t, J = 8.0 Hz, 6H, alkyl-H); MS (FAB): m/z (%) calcd for $\text{C}_{43}\text{H}_{74}\text{N}_2\text{O}_2$: 650.58 $[M]^+$; found: 650.9 (100) $[M]^+$.

3b: A solution of 2,2-diethylmalonyl chloride (0.86 mL, 5.00 mmol) in CH_2Cl_2 (40 mL) was added dropwise to a solution of pyrrole (0.687 g, 10.2 mmol) and aluminum chloride (1.37 g, 10.3 mmol) in CH_2Cl_2 (160 mL) over 10 min and stirred at room temperature. After monitoring of the consumption of the pyrrole by TLC, the mixture was poured into ice and extracted with CH_2Cl_2 . The organic layer was washed with brine and dried over anhydrous Na_2SO_4 . The solvent was removed by evaporation, and the residue was purified by chromatography and recrystallized from CH_2Cl_2 /hexane to give **3b** in 2% yield. R_f = 0.51 (5% MeOH/ CH_2Cl_2); ^1H NMR (400 MHz, CDCl_3 , 27°C): δ = 9.27 (brs, 2H, NH), 6.89 (m, 2H, pyrrole-H), 6.68 (m, 2H, pyrrole-H), 6.11 (m, 2H, pyrrole-H), 2.25 (q, J = 7.6 Hz, 4H, CH_2), 0.72 ppm (t, J = 7.6 Hz, 6H, CH_3); MS (FAB): m/z (%) calcd for $\text{C}_{15}\text{H}_{18}\text{N}_2\text{O}_2$: 258.14 $[M]^+$; found: 258.2 (71) $[M]^+$, 259.2 (100) $[M+1]^+$. This compound was further characterized by X-ray diffraction analysis.

Single-Crystal X-ray Diffraction Analysis

Data was collected on a Rigaku RAXIS-RAPID diffractometer for **1a** and **1d** and a Bruker SMART CCD diffractometer for **3a**, **3b**, and **4b** (Table 1), and refined by full-matrix least-squares procedures with anisotropic thermal parameters for the non-hydrogen atoms. The hydrogen atoms were calculated in ideal positions. Solutions of the structures were performed by using the Crystal Structure crystallographic software package (Molecular Structure Corporation) for **1a** and **1d** and Bruker SHELXTL for **3a**, **3b**, and **4b**. Crystals of **1a**, **1d**, **3a**, **3b**, and **4b** were obtained by vapor diffusion of hexane into a solution of these diketones in CH_2Cl_2 . CCDC-297709, 626137, and 297710–297712 (**1a**, **1d**, **3a**, **3b**, and **4b**, respectively) contain the supplementary crystallographic data for this paper. These data can be obtained free of charge from the Cambridge Crystallographic Data Centre at www.ccdc.cam.ac.uk/data_request/cif.

Electron, Optical, and Atomic Force Microscopy Studies

SEM images were obtained with a HITACHI S-4800 scanning electron microscope at acceleration voltages of 15 kV. Silicon (100) was used as substrate and a platinum coating was applied by using a HITACHI E-1030 Ion Sputterer unless otherwise stated. TEM images were obtained with a JEOL model JEM-1010 transmission electron microscope and STEM images were obtained with a HITACHI S-4800 scanning electron microscope. One drop of a solution of the materials was deposited on a carbon-coated copper grid (Ouken Shoji, Elastic Carbon coated Cu 200 Å mesh) and left to dry under high vacuum, and the observation was performed at room temperature at a voltage of 100 kV for TEM and 30 kV for STEM. No staining was used. OM images were captured with an Olympus BX51 microscope equipped with an MP5Mc/OL digital camera. AFM measurements were carried out with an SII EPA-400 instrument with an SPI 4000 Probe Station in dynamic force mode (tapping mode).

XRD analysis

XRD measurements were examined with a RIGAKU RINT Ultima III X-ray diffractometer. Solutions of the diketones in CH_2Cl_2 or n -hexane were dropped onto a glass plate for XRD and left to dry under high vacuum, and the observations were performed at room temperature.

Acknowledgements

This work was supported by a Grant-in-Aid for Young Scientists (B) (No. 17750137) from the Ministry of Education, Culture, Sports, Science, and Technology (MEXT), the Iketani Science Technology Foundation,

the Nissan Science Foundation, and the “Academic Frontier” Project for Private Universities, which is a matching fund subsidy from MEXT, 2003–2008 (H.M.). We thank Prof. Atsuhiko Osuka, Mr. Soji Shimizu, Mr. Shigeki Mori, and Mr. Shohei Saito, Kyoto University, for the X-ray analysis, Dr. Kazuko Fujii, NIMS, for help with XRD analysis, and Prof. Hitoshi Tamiaki, Ritsumeikan University, for helpful discussions.

- [1] a) *Current Challenges on Large Supramolecular Assemblies* (Ed.: G. Tsoucaris), NATO Science Series, Kluwer, Dordrecht, **1999**; b) *Supramolecular Polymers* (Ed.: A. Ciferri), Marcel Dekker, New York, **2000**; c) G. A. Ozin, A. C. Arsenault, *Nanochemistry: A Chemical Approach to Nanomaterials*, RSC, Cambridge, **2005**; d) *Topics in Current Chemistry: Supramolecular Dye Chemistry* (Ed.: F. Würthner), Springer Verlag, Berlin, **2005**.
- [2] a) F. J. M. Hoebe, P. Jonkheijm, E. W. Meijer, A. P. H. J. Schenning, *Chem. Rev.* **2005**, *105*, 1491–1546; b) R. A. Koevoets, R. M. Versteegen, H. Koojiman, A. L. Spek, R. P. Sijbesma, E. W. Meijer, *J. Am. Chem. Soc.* **2005**, *127*, 2999–3003; c) T. Nakanishi, N. Miyashita, T. Michinobu, Y. Wakayama, T. Tsuruoka, K. Ariga, D. G. Kurth, *J. Am. Chem. Soc.* **2006**, *128*, 6328–6329.
- [3] T. Kato, N. Mizoshita, K. Kishimoto, *Angew. Chem.* **2006**, *118*, 44–74; *Angew. Chem. Int. Ed.* **2006**, *45*, 38–68.
- [4] a) *Topics in Current Chemistry: Low Molecular Mass Gelators* (Ed.: F. Fages), Springer Verlag, Berlin, **2005**; b) T. Kitahara, M. Shirakawa, S. Kawano, U. Beginn, N. Fujita, S. Shinkai, *J. Am. Chem. Soc.* **2005**, *127*, 14980–14981.
- [5] a) T. Shimizu, M. Kogiso, M. Masuda, *Nature* **1996**, *383*, 487–488; b) T. Shimizu, *Polym. J.* **2003**, *35*, 1–22; c) T. Shimizu, M. Matsuda, H. Minamikawa, *Chem. Rev.* **2005**, *105*, 1401–1443.
- [6] a) J. P. Hill, W. Jin, A. Kosaka, T. Fukushima, H. Ichihara, T. Shimomura, K. Ito, T. Hashizume, N. Ishii, T. Aida, *Science* **2004**, *304*, 1481–1483; b) W. Jin, T. Fukushima, M. Niki, A. Kosaka, N. Ishii, T. Aida, *Proc. Natl. Acad. Sci. USA* **2005**, *102*, 10801–10806; c) W. Jin, T. Fukushima, A. Kosaka, M. Niki, N. Ishii, T. Aida, *J. Am. Chem. Soc.* **2005**, *127*, 8284–8285; d) J. Motoyanagi, T. Fukushima, N. Ishii, T. Aida, *J. Am. Chem. Soc.* **2006**, *128*, 4220–4221.
- [7] a) J.-S. Hu, Y.-G. Guo, H.-P. Liang, L.-J. Wan, L. Jiang, *J. Am. Chem. Soc.* **2005**, *127*, 17090–17095; b) R. Ghosh, A. Chakraborty, D. K. Maiti, V. G. Puranik, *Org. Lett.* **2006**, *8*, 1061–1064; c) M. Seo, G. Seo, S. Y. Kim, *Angew. Chem.* **2006**, *118*, 6454–6458; *Angew. Chem. Int. Ed.* **2006**, *45*, 6306–6310.
- [8] L. J. Prins, P. Timmerman, D. N. Reinhoudt, *Angew. Chem.* **2001**, *113*, 2446–2492; *Angew. Chem. Int. Ed.* **2001**, *40*, 2381–2426.
- [9] *The Porphyrin Handbook* (Eds.: K. M. Kadish, K. M. Smith, R. Guillard), Academic Press, San Diego, **2000**.
- [10] a) J. L. Sessler, S. Camiolo, P. A. Gale, *Coord. Chem. Rev.* **2003**, *240*, 17–55; b) P. A. Gale, *Chem. Commun.* **2005**, 3761–3772.
- [11] a) J. L. Sessler, S. J. Weghorn, Y. Hiseada, V. Lynch, *Chem. Eur. J.* **1995**, *1*, 56–67; b) M. Scherer, J. L. Sessler, A. Gebauer, V. Lynch, *J. Org. Chem.* **1997**, *62*, 7877–7881; c) M. Scherer, J. L. Sessler, M. Moini, A. Gebauer, V. M. Lynch, *Chem. Eur. J.* **1998**, *4*, 152–158; d) J. L. Sessler, G. Berthon-Gelloz, P. A. Gale, S. Camiolo, E. V. Anslyn, P. Anzenbacher, Jr., H. Furuta, G. J. Kirkovits, V. M. Lynch, H. Maeda, P. Morosini, M. Scherer, J. Shriver, R. S. Zimmerman, *Polyhedron* **2003**, *22*, 2963–2983.
- [12] C. Schmuck, W. Wienand, *J. Am. Chem. Soc.* **2003**, *125*, 452–459.
- [13] H. Uno, S. Ito, M. Wada, H. Watanabe, M. Nagai, A. Hayashi, T. Murashima, N. Ono, *J. Chem. Soc. Perkin Trans. 1* **2000**, 4347–4355.
- [14] a) H. Maeda, Y. Kusunose, *Chem. Eur. J.* **2005**, *11*, 5661–5666; b) C. Fujimoto, Y. Kusunose, H. Maeda, *J. Org. Chem.* **2006**, *71*, 2389–2394; c) H. Maeda, Y. Ito, *Inorg. Chem.* **2006**, *45*, 8205–8210; d) H. Maeda, Y. Ito, Y. Kusunose, T. Nakanishi, *Chem. Commun.* **2007**, in press; e) H. Maeda, Y. Kusunose, Y. Mihashi, unpublished results.
- [15] B. Oddo, C. Dainotti, *Gazz. Chim. Ital.* **1912**, *42*, 716–726.
- [16] W. M. Stark, M. G. Baker, F. J. Leeper, P. R. Raithby, A. R. Battersby, *J. Chem. Soc. Perkin Trans. 1* **1988**, 1187–1201.
- [17] R. M. Silverstein, E. E. Ryskiewicz, C. Willard, *Org. Synth.* **1956**, *36*, 74–76.

- [18] R. L. Hinman, S. Theodoropoulos, *J. Org. Chem.* **1963**, 28, 3052–3058.
- [19] J. S. Yadav, B. V. Reddy, S. G. Kondaji, R. S. Rao, S. P. Kumar, *Tetrahedron Lett.* **2002**, 43, 8133–8135.
- [20] R. Greenhouse, C. Ramirez, *J. Org. Chem.* **1985**, 50, 2961–2965.
- [21] T. Nakanishi, W. Schmitt, T. Michinobu, D. G. Kurth, K. Ariga, *Chem. Commun.* **2005**, 5982–5984.
- [22] Gaussian 03 (Revision C.02), M. J. Frisch, G. W. Trucks, H. B. Schlegel, G. E. Scuseria, M. A. Robb, J. R. Cheeseman, J. A. Montgomery, Jr., T. Vreven, K. N. Kudin, J. C. Burant, J. M. Millam, S. S. Iyengar, J. Tomasi, V. Barone, B. Mennucci, M. Cossi, G. Scalmani, N. Rega, G. A. Petersson, H. Nakatsuji, M. Hada, M. Ehara, K. Toyota, R. Fukuda, J. Hasegawa, M. Ishida, T. Nakajima, Y. Honda, O. Kitao, H. Nakai, M. Klene, X. Li, J. E. Knox, H. P. Hratchian, J. B. Cross, C. Adamo, J. Jaramillo, R. Gomperts, R. E. Stratmann, O. Yazyev, A. J. Austin, R. Cammi, C. Pomelli, J. W. Ochterski, P. Y. Ayala, K. Morokuma, G. A. Voth, P. Salvador, J. J. Dannenberg, V. G. Zakrzewski, S. Dapprich, A. D. Daniels, M. C. Strain, O. Farkas, D. K. Malick, A. D. Rabuck, K. Raghavachari, J. B. Foresman, J. V. Ortiz, Q. Cui, A. G. Baboul, S. Clifford, J. Cioslowski, B. B. Stefanov, G. Liu, A. Liashenko, P. Piskorz, I. Komaromi, R. L. Martin, D. J. Fox, T. Keith, M. A. Al-Laham, C. Y. Peng, A. Nanayakkara, M. Challacombe, P. M. W. Gill, B. Johnson, W. Chen, M. W. Wong, C. Gonzalez, J. A. Pople, Gaussian, Inc., Wallingford, **2004**.

Received: November 15, 2006
Published online: January 22, 2007